Journal of Alloys and Compounds 562 (2013) 116–122

Contents lists available at SciVerse ScienceDirect

Journal of Alloys and Compounds

journal homepage: www.elsevier.com/locate/jalcom

Effect of annealing processes on the structural and electrical properties of the lead-free thin films of $(Ba_{0.9}Ca_{0.1})(Ti_{0.9}Zr_{0.1})O_3$

Min Shi *, Jiagang Zhong, Ruzhong Zuo, Yudong Xu, Lei Wang, Hailin Su, Cang Gu

School of Materials Science and Engineering, Hefei University of Technology, Hefei, Anhui 230009, People's Republic of China

ARTICLE INFO

Article history:
Received 8 January 2013
Received in revised form 7 February 2013
Accepted 8 February 2013
Available online 19 February 2013

Keywords:
Sol–gel method
Annealing process
Lead-free ferroelectric thin films
Ferroelectric properties
Dielectric properties

ABSTRACT

Lead-free thin films of $(Ba_{0.9}Ca_{0.1})(Ti_{0.9}Zr_{0.1})O_3$ (BCZT) were prepared on $Pt/Ti/SiO_2/Si$ substrates by using sol–gel under three different annealing processes. Under the complex annealing process (CAP), the thin film is composed of a single phase with no trace of secondary phases, well crystallized and has a preferred orientation of (1 0 0). The thin film exhibits homogeneous polycrystalline grains without cracks and pores. The surface of the thin film has smooth surface with a root-mean-square (RMS) roughness of 5.67 nm. The interface between the thin film and the substrate is clear and smooth. The dielectric constant and the remnant polarization of the thin film prepared under CAP are greater than those prepared under the other annealing processes. But the dielectric loss and the coercive field are smaller. These results indicate that, among the three annealing processes, CAP is the best for preparing thin film of BCZT with good properties.

1. Introduction

Lead-based ferroelectric materials, such as $Pb(Zr,Ti)O_3$(PZT), have been widely used in ferroelectric random access memory, dynamic random access memory, micro-actuator, micro-sensor applications and high-power transducers owing to their excellent ferroelectric and piezoelectric properties [1–3]. Nevertheless, the main constituent element of these materials is lead [4]. Lead is a very toxic substance that can pollute environment, cause damage to brain and nervous system [5,6]. Therefore, in view of environmental protection and human health, it is urgent to develop lead-free ferroelectric materials [7]. In 2009, one of the most promising lead-free ferroelectric systems, Ca and Zr doped $BaTiO_3$ (BCZT) which exhibits excellent piezoelectric behavior (d33 ≈ 620pC/N) was reported by Liu and Ren [8]. He pointed out that doping amount of Ca and Zr will influence the piezoelectric behavior of BCZT. Mahajan et al. [9] also pointed out that it will increase the ferroelectric properties by doping Ca and Zr in $BaTiO_3$-based materials. Wu et al. [10–12] obtained enhanced piezoelectric properties in $(Ba_{0.85}Ca_{0.15})(Ti_{0.9}Zr_{0.1})O_3$ ceramics. Li et al. [13] obtained high piezoelectric coefficient in $(Ba_{0.99}Ca_{0.01})(Ti_{0.98}Zr_{0.02})O_3 + x$ mol% ($x = 0–0.8$) Yttrium ceramics by solid-state technique. However, the researches on BCZT are almost focused on bulk ceramics. There is lack of research reported on thin films of BCZT.

To date, ferroelectric thin films were mainly prepared by physical methods (e.g., pulsed laser deposition and radio frequency sputtering) [14,15] and chemical solution deposition method (e.g., sol–gel method) [16]. By physical methods, the surfaces of ferroelectric thin films are very compact, and the piezoelectric effects of thin films materials are great. However, these methods require expensive laboratory equipment and high vacuum, critical control over processing condition, high cost and long deposition time. Among the chemical solution deposition methods, the sol–gel method has several advantages such as the precise control of chemical composition, low processing temperature, low cost, deposition in air not under vacuum atmosphere. Nevertheless, the annealing processes will influence the crystallographic phase, microstructure and electrical properties of the resultant thin films [17–19]. Therefore further investigations into the optimization of the various annealing processes are required to improve the ferroelectric and dielectric properties of the thin films of BCZT.

In this work, the lead-free thin films of $(Ba_{0.9}Ca_{0.1})(Ti_{0.9}Zr_{0.1})O_3$ (BCZT) were deposited on $Pt/Ti/SiO_2/Si$ substrates using sol–gel and spin-coating method. In order to investigate the influence of different annealing conditions on the structures and properties of the thin films of BCZT, we chose three different annealing processes. The effects of three annealing processes on the microstructure, dielectric properties and ferroelectric properties of the thin films of BCZT were investigated in detail. The optimized annealing process for preparing thin film of BCZT was also determined.

2. Experimental

Synthesis of the films of BCZT relies on the preparation of stable precursor sol. Precursor sol of BCZT was prepared by the sol–gel method. Barium acetate $(Ba(CH_3COO)_2)$, calcium acetate $(Ca(CH_3COO)_2)$, zirconium (IV) isopropoxide

* Corresponding author. Tel./fax: +86 551 62901362.
E-mail address: mrshimindou@hotmail.com (M. Shi).

0925-8388/$ - see front matter © 2013 Elsevier B.V. All rights reserved.
http://dx.doi.org/10.1016/j.jallcom.2013.02.054

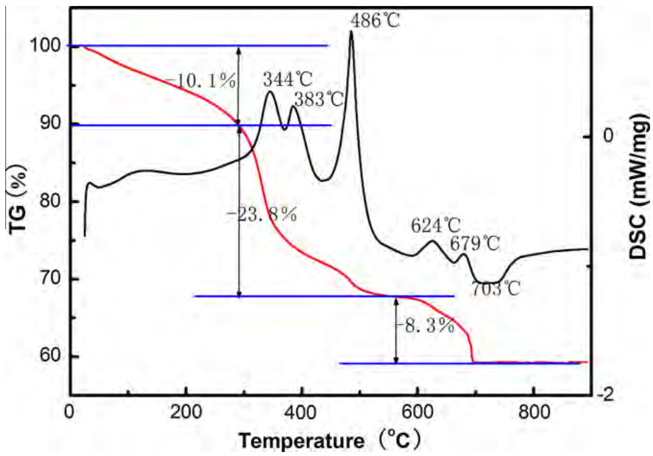

Fig. 1. TG and DSC curves of the BCZT precursor gel.

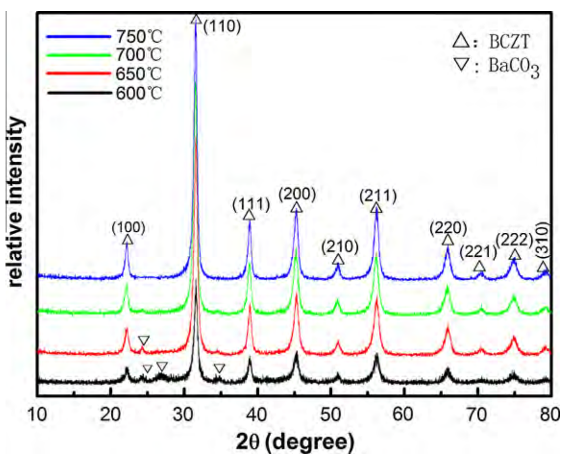

Fig. 2. XRD patterns of BCZT powders annealed at different temperatures.

($Zr(OC_3H_7)_4$) and terabutyl titanate ($Ti(OC_4H_9)_4$) were used as starting materials. Glacial acetic acid (CH_3COOH) and ethylene glycol monomethyl ether ($HOCH_2CH_2OCH_3$) were used as a solvent. According to the stoichiometric ratio of $(Ba_{0.9}Ca_{0.1})(Ti_{0.9}Zr_{0.1})O_3$, firstly, terabutyl titanate was dissolved in the ethylene glycol monomethyl. Zirconium (IV) isopropoxide was then added at 60 °C with continuous stirring for 30 min. A stoichiometric amount of the barium acetate and calcium acetate were dissolved in glacial acetic acid, stirred at 60 °C until dissolved completely. The above two solutions were mixed with continuous stirring at 60 °C for 2 h to obtain a stable precursor sol of BCZT. The precursor sols of BCZT were dried at 100 °C for 12 h to prepare BCZT powders for the XRD analysis. The thin films of BCZT were formed by spin-coating the sols of BCZT onto the $Pt/Ti/SiO_2/Si$ substrates at 500 rpm for 9 s and 3300 rpm for 30 s. The processes of spin-coating were repeated several times to increase thicknesses of the thin films. In order to reduce the thermal stresses resulted from the thermal decompositions of various organic compounds and prepare the well-crystallized films with high phase purity, the thin films need to be pre-annealed and annealed. The temperatures of pre-annealing and annealing were determined by the results of the thermal analysis and XRD, respectively. In order to investigate the effects of annealing processes on the structure and properties of materials, the films were prepared under three different annealing processes.

The simple annealing process (SAP) is as follows: firstly, the BCZT sols were spin-coated on the $Pt/Ti/SiO_2/Si$ substrates to obtain one-layered thin film of BCZT. Then, treatments of spin-coating were repeated several times to obtain the multilayer thin films of BCZT. Finally, the thin films were pre-annealed at 500 °C for 10 min and annealed at 700 °C for 20 min. Under SAP, the thin films of BCZT were prepared after one pre-annealing process and one annealing process.

The ordinary annealing process (OAP) is as follows: firstly, the BCZT sols were spin-coated on the substrates to obtain one-layer thin film of BCZT. The thin films were pre-annealed at 500 °C for 10 min. Then the treatments of spin-coating and pre-annealing were repeated two times to obtain the multilayer films. Finally, the multilayer films were annealed at 700 °C for 20 min. The thin films of BCZT have the desired thickness of ~120 nm. Under OAP, the thin films of BCZT were prepared after three pre-annealing processes and one annealing process.

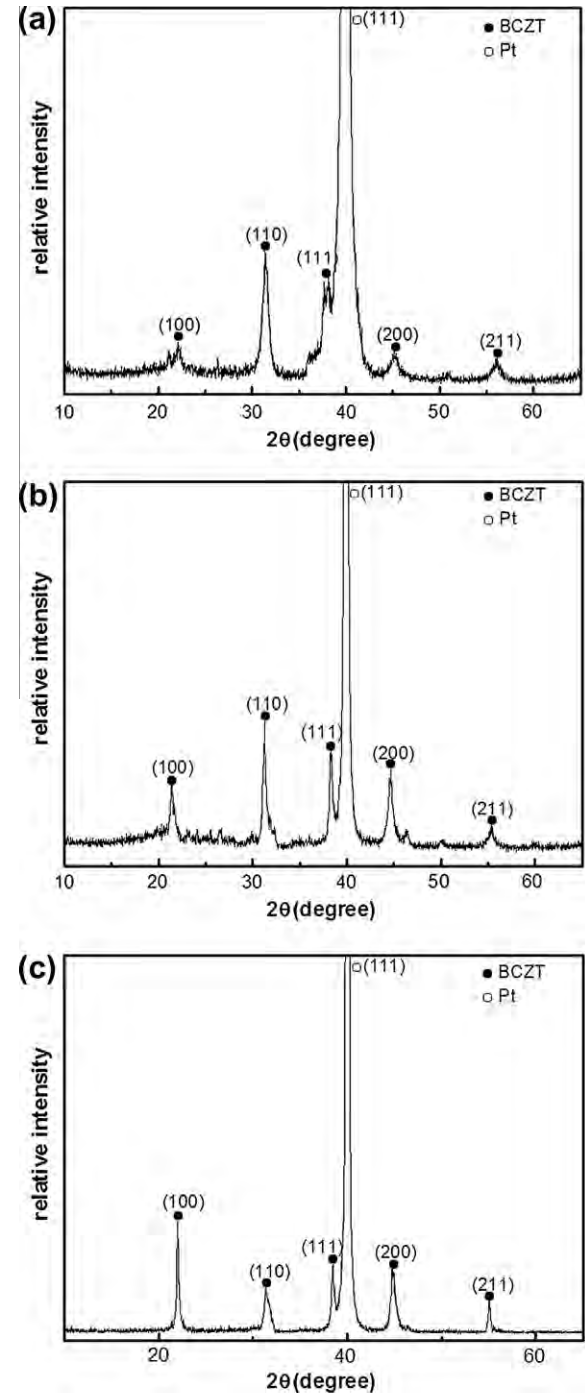

Fig. 3. XRD patterns of BCZT thin films prepared under different annealing processes; (a) SAP, (b) OAP and (c) CAP.

The complex annealing process (CAP) is as follows: firstly, the sols of BCZT were spin-coated on the substrates to obtain one-layered thin film of BCZT. Then, the thin films were pre-annealed at 500 °C for 10 min and annealed at 700 °C for 20 min. The processes of spin-coating, pre-annealing and annealing treatment were then repeated two times to obtain the multilayer films. The thin films of BCZT have the desired thickness of ~120 nm. Under CAP, the thin films of BCZT were prepared after three pre-annealing and annealing processes.

Both thermo-gravitometry (TG) and differential scanning calorimetry (DSC) analysis of the gels of BCZT were carried out using a simultaneous thermal analyzer (STA409C, Netzsch, Germany). The phase compositions and crystallographic structures of the powders and the thin films were performed by using an X-ray diffraction (D/MAX2500 VL/PC, Rigaku, Japan). The surfaces and the cross-sections of the thin films of BCZT were observed with a field-emission scanning electron microscope (FE-SEM, Sirion200, FEI, USA). The surface microstructures and roughnesses of the thin films were characterized by an atomic force microscope (AFM, SPA-300HV Seiko, Japan). The polarization versus electric field (P–E) hysteresis loops were characterized using a ferroelectric tester (Precision LC, Radiant Technologies, Inc., USA).The dielectric properties (dielectric constant and dielectric loss) were measured by LCR meter (Agilent, 4980A, USA). Before the electrical measures, Ag electrodes with a diameter of 150 μm were deposited through a shadow mask on the thin films.

3. Results and discussions

Thermo-gravitometry (TG) and differential scanning calorimetry (DSC) analysis of the precursor gel of BCZT is presented in Fig. 1. The weight loss of 10.1% at temperatures up to about 215 °C is due to the evaporation of organic solution. There exothermic peaks at 344 °C, 383 °C, 486 °C may be attributed to the combustion or thermal decomposition of various organic compounds, corresponding to a weight loss of 23.8%. There are two exothermic peaks at 624 °C, 679 °C, which could be probably attributed to the formation and crystallization of phase BCZT with a weight loss of 23.8%. In this work, based on results of thermal analysis, the BCZT thin films were pre-annealed at 500 °C to decompose various organic compounds in order to decrease thermal stresses in the films which are due to the film shrinkages resulted from the decompositions of organic compounds. Accordingly, the amount of cracks and pores in BCZT can be decreased. The final annealing temperature of thin films of BCZT should be above 679 °C or higher for obtaining the well-crystallized thin films of BCZT. An accurate annealing temperature of thin films of BCZT will be determined by the results of XRD.

Fig. 2 shows XRD patters of BCZT powders annealed at different temperatures. It is seen that all the BCZT powders annealed ranging from 600 °C to 750 °C have polycrystalline structures. When annealed at 600 °C, the powders contain a large amount of main phase, i.e. BCZT phase and a small amount of secondary phase, i.e. $BaCO_3$ phase. With the increase of annealing temperatures, the relative amounts of secondary phase decrease. It is apparent that there are no detectable secondary phases when the annealing temperature reached 700 °C or higher. For films and powders have similar characteristics under the same heat treatment condition, the annealing temperatures of powders can provide an important reference for films. The accurate annealing temperatures of films need to be determined by XRD results of films. Xu et al. [20,21] determined annealing temperature of films through referencing

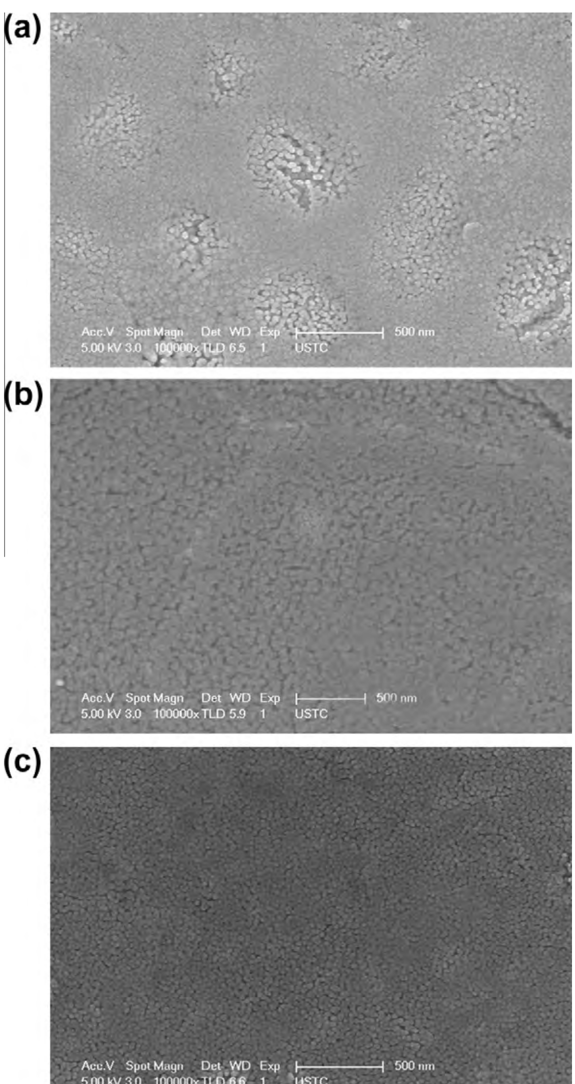

Fig. 4. SEM images of surfaces of BCZT films prepared under different annealing processes; (a) SAP, (b) OAP and (c) CAP.

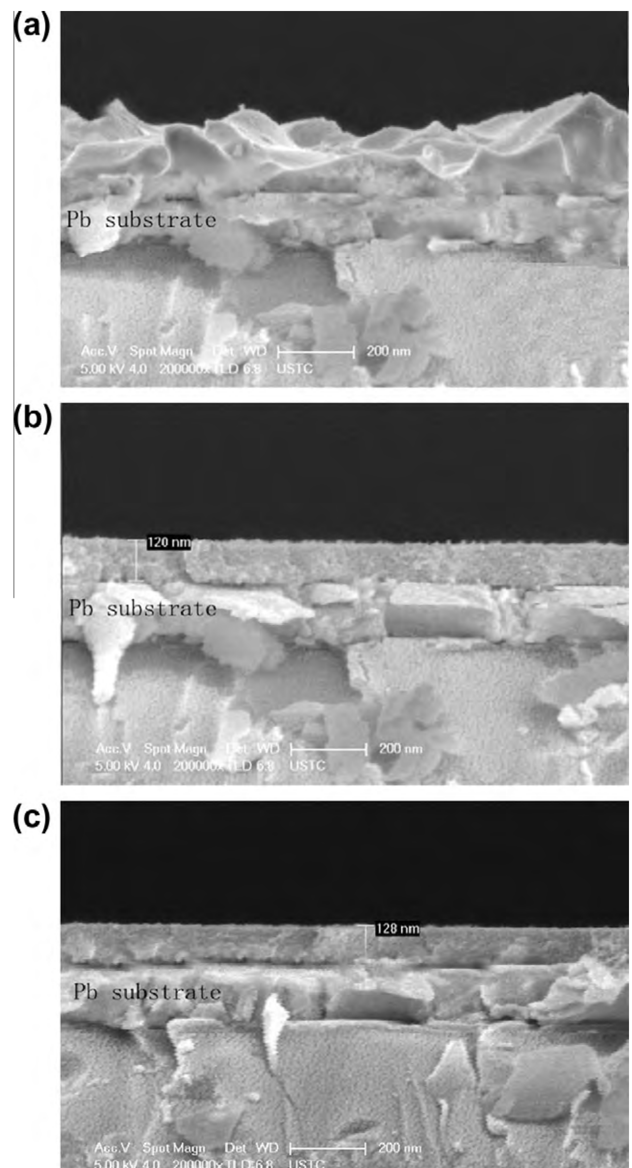

Fig. 5. SEM images of cross section of BCZT films prepared under different annealing processes; (a) SAP, (b) OAP and (c) CAP.

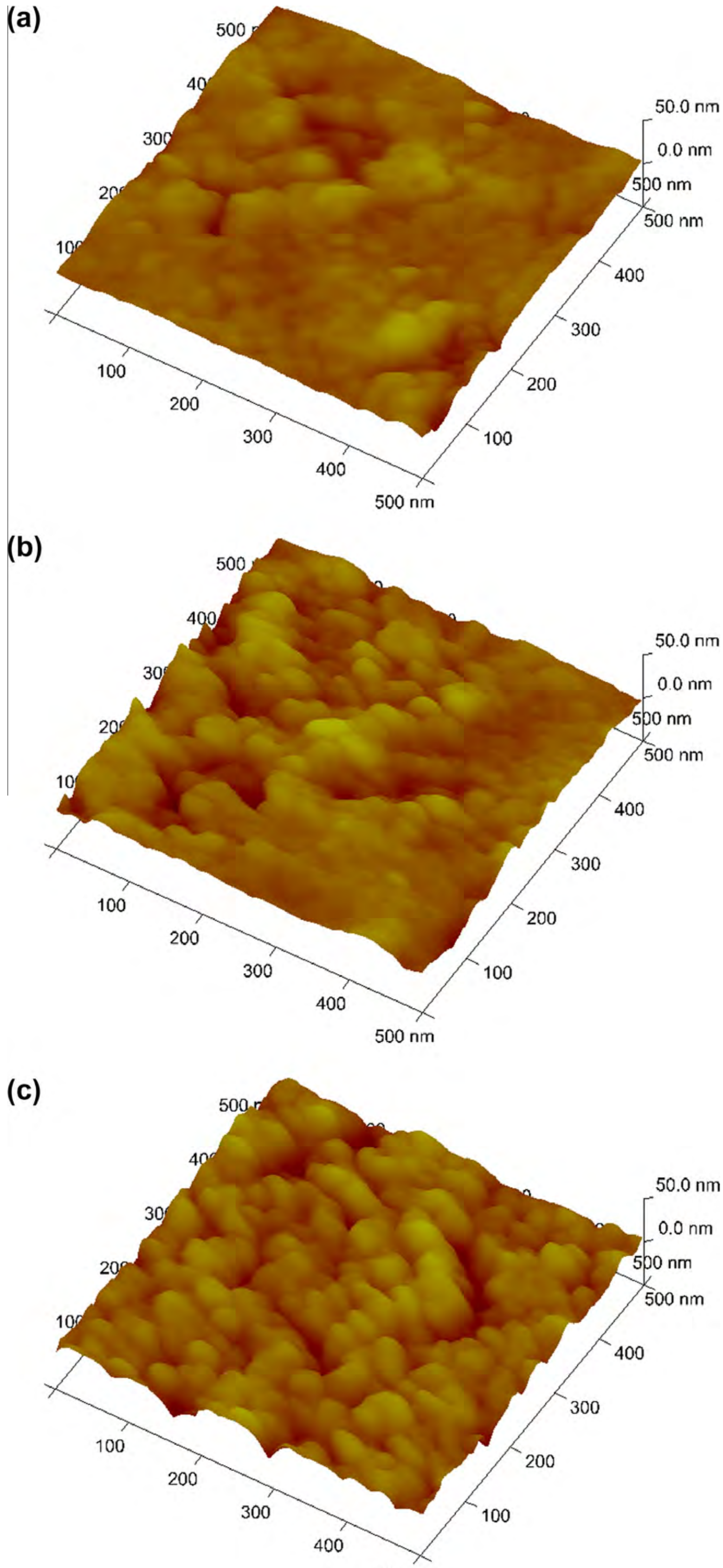

Fig. 6. AFM micrographs of the BCZT films prepared under different annealing processes; (a) SAP, (b) OAP and (c) CAP.

annealing temperature of powders. Consequently, with reference to XRD results of powders, the final annealing temperatures of the thin films of BCZT can be roughly set at ~700 °C.

In order to investigate the influences of different annealing processes on the structures of the thin films of BCZT, XRD analysis was used. The XRD patterns of the thin films of BCZT prepared under three different annealing processes are presented in Fig. 3. From Fig. 3a and b, it is obvious that the thin films of BCZT prepared under SAP and OAP contain a large amount of main phase, i.e. BCZT phase and Pt phase from the $Pt/Ti/SiO_2/Si$ substrate, a small amount of non-crystalline phase. The reason may be that the films are not fully pre-annealed or annealed. Therefore, organic compounds cannot be decomposed completely or the films cannot be well crystallized. It also indicates that there were no preferred orientations in the films. Nevertheless, from Fig. 3C, it is seen that, under CAP, the thin film of BCZT is composed of a single phase (BCZT) with no traces of secondary phases, well crystallized and has a preferred orientation of (1 0 0). A preferred orientation in the films will benefit the ferroelectric and dielectric properties of the thin films [22–26]. Based on the XRD results, it is concluded that, among the three annealing processes, CAP is the best for preparing the BCZT thin films with high phase purity and preferred orientation.

Fig. 4 exhibits SEM images of surfaces of the thin films of BCZT under different annealing processes. From Fig. 4a, it is seen that there exist obvious pores and cracks in the film prepared under SAP. Fig. 4b shows that, under OAP, the thin film contains smaller amount of cracks and pores. The reasons are as follows: in the films prepared under SAP and OAP, decompositions of organic compounds have not been completed. The stresses resulted from decompositions of remained organic compounds will lead to cracks and pores, when the films are annealed at 700 °C finally. Fig. 4c illustrates that thin films are dense and exhibit homogeneous polycrystalline grains without cracks and pores. This indicates that adverse effects of the decompositions of organic compounds in the thin films have been completely eliminated and crystallization has completed. Therefore, under CAP, the thin films of BCZT with good morphology can be prepared.

Fig. 5 exhibits SEM images of the cross-sections of the thin films of BCZT prepared under three different annealing processes. From Fig. 5a, it is seen that the surface of the thin film prepared under SAP is uneven and there is no obvious interface between the thin film and the substrate. This implies that the presence of diffusion between the thin film and the substrate at the interface. Nevertheless, this diffusion will deteriorate dielectric and ferroelectric properties of the thin film. Therefore, for ferroelectric materials, the diffusion at the interface should to be avoided. Fig. 5b and c reveals that the surfaces of the thin films prepared under OAP and CAP are very smooth, the interfaces between the thin films and the substrates are clear and smooth. This suggests that there are no diffusions between the thin films of BCZT and the substrates at the interface. The thicknesses of thin films prepared under OAP and CAP are approximately 120 nm and 128 nm, respectively.

Fig. 6 presents the AFM topography images of the thin films of BCZT prepared under the three different annealing processes. It can be seen that the film prepared under SAP has pores and no obvious grain. The film prepared under OAP has small amount of pores and grains. Nevertheless, the film prepared under CAP has a dense and pore-free surface, and the grains exhibit sphere-shape. The surface of the thin film prepared under CAP has a root-mean-square (RMS) roughness of 5.67 nm. Small RMS roughness of the film surface means that the film has a smooth surface.

The dielectric losses of BCZT thin films, prepared under three annealing processes, measured as function of frequency at room temperature, are shown in Fig. 7. For the thin films prepared under three annealing processes, when the frequency is lower than 10,000 Hz, dielectric losses decrease rapidly with increasing frequency. When the frequency is between 10,000 Hz and 60,000 Hz, dielectric losses decrease slowly. When the frequency is higher than 60,000 Hz, dielectric losses remain almost unchanged. This is in agreement with results of Wu et al. [10,27]. At the same frequency, dielectric loss of thin film prepared under CAP is slightly smaller than that of thin film prepared under OAP. They are all much smaller that of thin film prepared under SAP. This can be attributed to cracks, pores or secondary phases in the thin films prepared under SAP. The dielectric constants of thin films of BCZT prepared under three annealing processes are displayed in Fig. 8. For the thin films prepared under three annealing processes, when the frequency is lower than 8000 Hz, the dielectric constants decrease rapidly with increasing frequency. When the frequency is between 8000 Hz and 60,000 Hz, the dielectric constants decrease slowly. When the frequency is higher than 60,000 Hz, the dielectric constants remain almost unchanged. At lower frequency (<about 8000 Hz), the dielectric constant of thin film prepared under CAP is close to those prepared under the other two annealing processes. Nevertheless, at high frequency (>10,000 Hz), the dielectric constant of the thin film prepared under CAP exceeds those prepared under SAP and OAP. This may be attributed to the preferred orientation of (1 0 0) in the thin film prepared under CAP [22,28,29].

Polarization–electric hysteresis loops (P–E) of thin films of BCZT prepared under three annealing processes were measured under

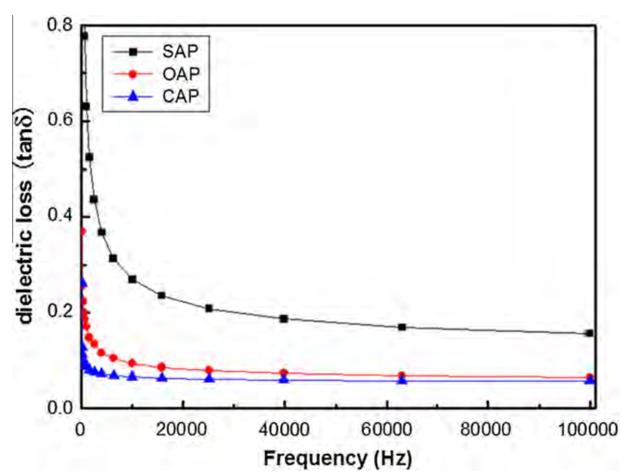

Fig. 7. Frequency dependence of dielectric losses of BCZT thin films prepared under different annealing processes.

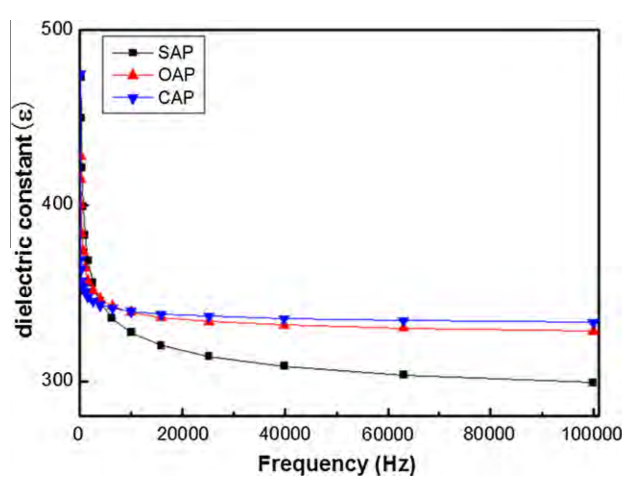

Fig. 8. Frequency dependence of dielectric constants of BCZT thin films prepared under different annealing processes.

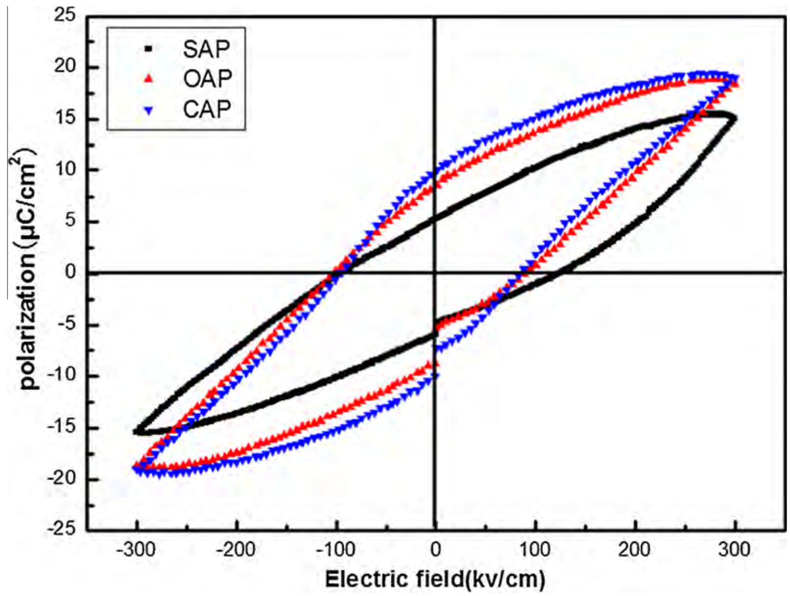

Fig. 9. P–E hysteresis loops of the BCZT thin films prepared under different annealing processes at an applied maximum electric field of 300 kV/cm.

Table 1
The remnant polarization (P_r) and the coercive fields (E_c) of thin films of BCZT prepared under different annealing processes drawn from Fig. 8.

The thin film prepared under	P_r (μC/cm^2)	E_c (kV/cm)
SAP	3.42	106.57
OAP	8.60	92.82
CAP	10.08	88.23

different electric fields, as shown in Fig. 9. All the thin films exhibit typical ferroelectric behavior under an applied maximum electric field of 300 kV/cm. It shows that the P–E loops do not reach saturation. The results drawn from Fig. 8 were listed in Table 1. It is seen that the remnant polarization (P_r) of the film prepared under CAP is greater than those of the prepared under SAP and OAP. This can be due to preferred orientation of (100) in the film prepared under CAP. The remnant polarization of the film prepared under CAP is 10.08 μC/cm^2, which is greater than those of ferroelectric thin films prepared by sol–gel method in Refs. [30,31]. It can also be seen that the coercive fields (E_c) of the film prepared under CAP is smaller than those prepared SAP and OAP. This can be attributed to existence of cracks and pores, which restrict the movements of domains in the thin films prepared under SAP and OAP. By summarizing the experimental results, we can conclude that CAP is the best for preparing thin films of BCZT with good ferroelectric and dielectric properties.

4. Conclusions

In this work, the lead-free thin films of BCZT have been successfully prepared by the sol–gel and spin-coating method on the Pt/Ti/SiO_2/Si substrate. The thin films were treated under three different annealing processes. Under CAP, the thin films of BCZT are composed of a single phase (BCZT), well crystallized and have a preferred orientation of (100). High phase purity and preferred orientation will help to increase ferroelectric properties; the interface between the thin film and substrate is clear and smooth, implying that there is no diffusion between the thin film and the substrate; the thin films exhibit homogeneous polycrystalline grains without cracks and pores. The dielectric constant and the remnant polarization of the thin film prepared under CAP are greater than those prepared under the other two annealing processes. Nevertheless, the dielectric loss and the coercive field are smaller. It is concluded that, among the three annealing processes, CAP is the best for preparing thin films of BCZT with good properties.

Acknowledgements

The authors wish to acknowledge the financial support of this research from Anhui Provincial Natural Science Foundation and Nippon Sheet Glass Foundation for Materials Science and Engineering (Japan).

References

[1] Y.T. Pu, J.L. Zhu, X.H. Zhu, Y.S. Luo, X.D. Li, M.S. Wang, J. Liu, X.H. Li, J.G. Zhu, D.Q. Xiao, Ceram. Int. 38 (2012) S233.
[2] P. Khare, D. Sa, Solid State Commun. 152 (2012) 1572.
[3] G.H. Haertling, J. Am. Ceram. Soc. 82 (1999) 797.
[4] D. Fasquelle, M. Mascot, J.C. Carru, Solid-State Electron. 75 (2012) 6.
[5] Y. Saito, H. Takao, T. Tani, T. Nonoyama, K. Takatori, T. Homma, T. Nagaya, M. Nakamura, Nature 432 (2004) 84.
[6] C.Y. Kim, T. Sekino, K. Niihara, J. Sol–Gel Sci. Technol. 55 (2010) 306.
[7] T.R. Shrout, S.J. Zhang, J. Electroceram. 19 (2007) 113.
[8] W.F. Liu, X.B. Ren, Phys. Rev. Lett. 103 (2009) 257602.
[9] S. Mahajan, O.P. Thakur, D.K. Bhattacharya, K. Sreenivas, Mater. Chem. Phys. 112 (2008) 858.
[10] J.G. Wu, D.Q. Xiao, W.J. Wu, J.G. Zhu, J. Wang, J. Alloys Comp. 509 (2011) L359.
[11] J.G. Wu, D.Q. Xiao, W.J. Wu, Q. Chen, J.G. Zhu, Z.C. Yang, J. Wang, Scr. Mater. 65 (2011) 771.
[12] J.G. Wu, D.Q. Xiao, W.J. Wu, Q. Chen, J.G. Zhu, Z.C. Yang, J. Wang, J. Eur. Ceram. Soc. 32 (2012) 891.
[13] W. Li, J.G. Hao, W.F. Bai, Z.J. Xu, R.Q. Chu, J.W. Zhai, J. Alloys Comp. 531 (2012) 46.
[14] D.Y. Wang, D.M. Lin, K.W. Kwok, N.Y. Chan, J.Y. Dai, S. Li, H.L.W. Chan, Appl. Phys. Lett. 98 (2011) 022902.
[15] D.Y. Wang, N.Y. Chan, S. Li, S.H. Choy, H.Y. Tian, L.W. Chan Helen, Appl. Phys. Lett. 97 (2010) 212901.
[16] T. Matsuda, W. Sakamoto, B.Y. Lee, T. Lijima, J. Kumagai, M. Moriya, T. Yogo, Jpn. J. Appl. Phys. 51 (2012) 09LA03.
[17] J. Ihlefeld, B. Lauglhin, A. Hunt-Lowery, W. Borland, A. Kingon, J.P. Maria, J. Electroceram. 14 (2005) 95.
[18] B. Malic, I. Boerasu, M. Mandeljc, M. Kosec, V. Sherman, T. Yamada, N. Setter, M. Vukadinovic, J. Eur. Ceram. Soc. 27 (2007) 2945.
[19] D.M. Tahan, A. Safari, L.C. Klien, J. Am. Ceram. Soc. 79 (1996) 1593.
[20] Y.D. Xu, G. Wu, H.L. Su, M. Shi, G.Y. Yu, L. Wang, J. Alloys Comp. 509 (2011) 3811.
[21] L. Wang, R.Z. Zuo, L.D. Liu, H.L. Su, M. Shi, X.C. Chu, X.H. Wang, L.T. Li, Mater. Chem. Phys. 130 (2011) 165.

[22] M.H. Lee, J.S. Park, D.J. Kim, H.J. Cho, Y.S. Sung, M.H. Kim, J.H. Cho, H.I. Choi, D. Do, W.J. Kim, S.S. Kim, B.C. Choi, T.K. Song, Curr. Appl. Phys. 11 (2011) S189.
[23] J. Ventura, I. Fina, C. Ferrater, E. Langenberg, L.E. Coy, M.C. Polo, M.V. Garcia-Cuenca, L. Fabrega, M. Varela, Thin Solid Films 518 (2010) 4692.
[24] D. Ambika, V. Kumar, H. Imai, I. Kanno, K. Isaku, Appl. Phys. Lett. 96 (2010) 031909.
[25] J.W. Zhai, X. Yao, L.Y. Zhang, B. Shen, C. Haydn, J. Cryst. Growth 1–4 (2004) 341.
[26] J.W. Zhai, C. Gao, X. Yao, Z.K. Xu, C. Haydn, Ceram. Int. 34 (2008) 905.
[27] L.G.A. Marques, L.S. Cavalcante, A.Z. Simoes, F.M. Pontes, L.S. Santos-Junior, M.R.M.C. Santos, I.L.V. Rosa, J.A. Varela, E. Longo, Mater. Chem. Phys. 105 (2007) 293.
[28] S.Q. Zhang, L.D. Wang, L.W. Li, N. Li, W.D. Fei, J. Alloys Comp. 509 (2011) 2976.
[29] M.C. Kao, H.Z. Chen, S.L. Young, B.N. Chuang, W.W. Jiang, J.S. Song, S.S. Jhan, J.L. Chiang, L.T. Wu, J. Cryst. Growth 338 (2012) 139.
[30] Y.H. Fan, S.H. Yu, R. Sun, L. Li, Y.S. Yin, R.X. Du, Thin solid films 518 (2010) 3610.
[31] M. Kumar, S. Rani, M.C. Bhatnagar, S.C. Roy, Mater. Chem. Phys. 2–3 (2008) 399.